ACS Macro Letters

pubs.acs.org/macroletters Letter

Bilayer Hydrogels by Reactive-Induced Macrophase Separation

Dong Zhang, Yijing Tang, Xiaomin He, William Gross, Jintao Yang, and Jie Zheng*

Cite This: ACS Macro Lett. 2023, 12, 598−604 Read Online

ACCESS | Metrics & More | Article Recommendations | * Supporting Information

ABSTRACT: Bilayer hydrogels encoded with smart functions have emerged as promising soft materials for engineered biological tissues and human-machine interfaces, due to the versatility and flexibility in designing their mechanical and chemical properties. However, conventional fabrication strategies often require multiple complicated steps to create an anisotropic bilayer structure with poor interfaces, which significantly limit the scope of bilayer hydrogel applications. Here, we reported a general, one-pot, macrophase separation strategy to fabricate a family of bilayer hydrogels made of vinyl and styryl monomers with a seamless interface and a controllable layer separation eficiency (20−99%). The working principle of a macrophase separation strategy allows for the decoupling of the two gelation processes to form distinct vinyl- and styryl-enriched layers by manipulating competitive polymerization reactions between vinyl and styryl monomers. This work presents a straightforward approach and a diverse range of radical monomers, which can be utilized to create next-generation bilayer hydrogels, beyond a few available today.

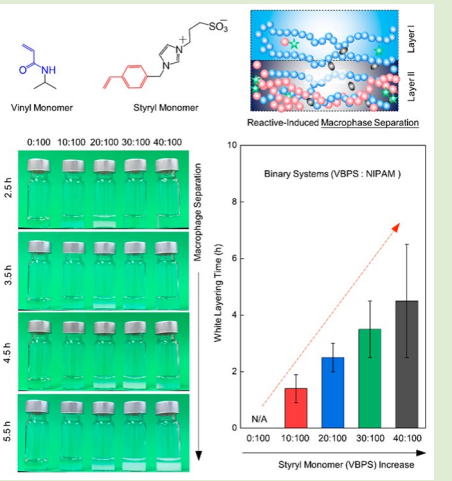

Bilayer hydrogels have emerged as promising smart soft materials encoded with programmable stimuli-responsive functions to achieve built-on-demand shape transformation and morphing for different advanced applications in artificial muscles, soft electronics, and human−machine interfaces.[1−10] As compared to single-layer hydrogels with isotropic or homogeneous network structures, bilayer hydrogels offer structural and functional advantages for realizing superior spatiotemporal actuations (e.g., shape transformation, movements, bending, and twisting) in a programmable manner when responding to external stimuli of pH, temperature, light, and external force fields. Achieving such hierarchical structures in bilayer hydrogels requires to integrate multiple cross-linked networks and stimuli-responsive polymers into the two immiscible phases at macro/mesoscales. However, the design of bilayer hydrogels with on-demand actuations and strong mechanical properties still presents a persistent challenge.

Conventional fabrication strategies for preparing bilayer hydrogels often involve the two- or multiple-step layer-by-layer polymerizations in a sequential order. Briefly, once the first hydrogel layer was formed via the first polymerization step, one side of the first layer was partially immersed into the second-layer precursor solution, followed by in situ polymerization to form the second layer on top of the first layer, with an interpenetrating network at the interface.[11−13] While this multistep, layer-by-layer polymerization strategy is straightforward and applicable to a wide range of monomers and cross-linkers to form bilayer hydrogels, the stepwise polymerizations have certain inherent disadvantages, i.e., the second-step polymerization requires the diffusion of second-layer precursors into the swollen first-layer hydrogel, during which swelling and diffusion processes happen spontaneously and cannot be precisely controlled, thus often leading to an uneven interpenetrating network and heterogeneous defects at the hydrogel interface. Consequently, such a structural mismatch at the bilayer interface is prone to limited actuations, slow response, weak interfacial bonding, and mechanical failures, in response to environmental stimuli. Since the interfacial adhesion and mechanical toughness are the two key prerequisites for the performance of bilayer hydrogels, several strategies have been proposed to enhance mechanical strength and interfacial bonding by introducing highly reversible bonds (e.g., ionic association, supramolecular assembly, host−guest interactions, hydrogen bonding). However, multistep, layer-by-layer polymerization strategies still encounter a challenge to control the bonding process for joining the two hydrogels together and forming a strong bilayer interface.

To address this bilayer interface issue from a fabrication perspective, developing a new, one-pot polymerization method to form bilayer hydrogels is probably the best strategy to mitigate as much of the issues of weak interfacial bonding and

Received: March 9, 2023
Accepted: April 10, 2023
Published: April 17, 2023

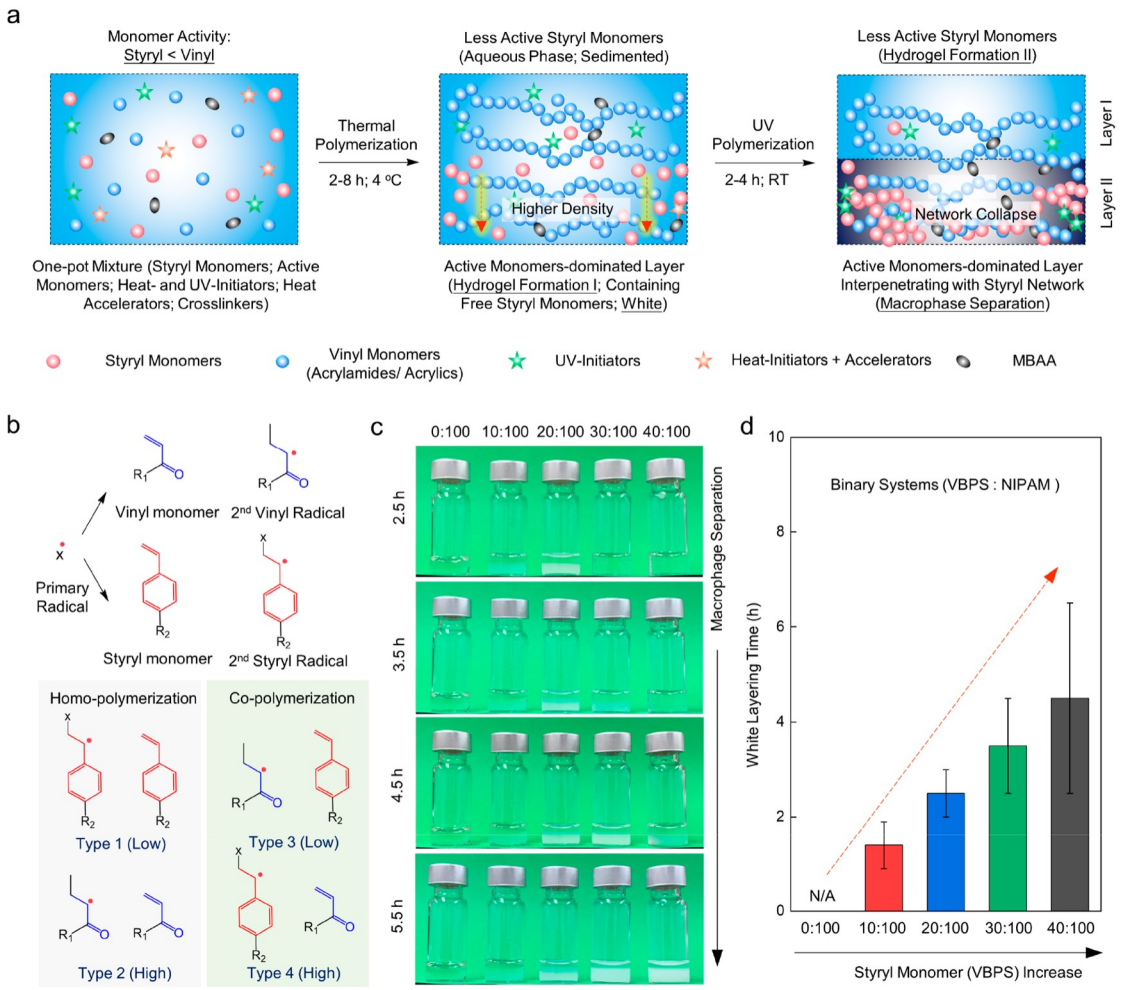

Figure 1. Fabrication of bilayer hydrogels via a radical-induced macrophase separation strategy. (a) Design strategy and general synthesis procedure of macrophase separation-induced bilayer hydrogels made of a vinyl-enriched layer and a styryl-enriched layer via one-pot, dual radical polymerizations. (b) Competitive radical reaction to initialize and grow vinyl- and styryl-based networks in two distinct layers. (c) Time-dependent snapshots of the entire gelation process of VBPS and NIPAM monomers. (d) Delamination time of pNIPAM-pVBPS bilayer hydrogels prepared with different VBPS:NIPAM mass ratios of 0:100, 10:100, 20:100, 30:100, and 40:100.

interfacial structural mismatch as possible while also ensuring responsive, programmable actuations, and strong mechanical properties. To achieve a bilayer structure by the one-pot polymerization/gelation methods, a potential working principle is to construct the two contrasting networks with incompatible physicochemical properties (e.g., hydrophobicity vs hydrophilicity, swelling vs nonswelling, polymer contraction vs polymer expansion, ionic repulsion vs ionic attraction). The one-pot methods have been used to prepare the two most typical bilayer hydrogels of (i) organogels and (ii) gradient hydrogels. Strictly speaking, bilayer organogels are not considered as pure hydrogels, instead they are formed by hydrophilic polymer networks infiltrated with organic solvents, followed by the separation of organic and aqueous phases into the two layers. This one-pot, bilayer fabrication is limited to specific polymers in organic solvents, because only polymers are qualified for cross-linking in organic solvents to form 3D networks. An alternative one-pot strategy is to prepare bilayer hydrogels with gradient structures by applying external fields/forces (electric, magnetic, gravitational, or centrifugal force) to drive different constituents to form two asymmetric layers. But, the gradient structures in bilayer hydrogels possess inhomogeneous and blurred layer-to-layer interfaces (i.e., pseudobilayer structure), which render dificult to achieve both mechanical strength and stimulus responsiveness simultaneously. Therefore, it still remains a great challenge for developing a new universal fabrication strategy, which can be applied to new polymer systems for preparing bilayer hydrogels with seamless interfaces and desirable mechanical and actuation functions.

Since little is known about how radical polymers work together for realizing bilayer hydrogels, we reported a conceptually macrophase separation strategy to prepare bilayer hydrogels by controlling the radical polymerization/gelation process in one-pot, binary reactive systems. To achieve this design, the two selected monomers, from a gelation viewpoint, should be compatible with each other for free-radical polymerization in the same precursor solution upon certain external stimuli. Meanwhile, the two polymerized polymers should be suficiently different in physicochemical properties to realize subsequent phase separation to form the two hydrogel layers. After prescreening through a range of different monomers, we identified a vinyl monomer and a zwitterionic styryl monomer for the preparation of bilayer hydrogels via the polymerization-induced macrophase separation mechanism.

https://doi.org/10.1021/acsmacrolett.3c00149
ACS Macro Lett. 2023, 12, 598−604

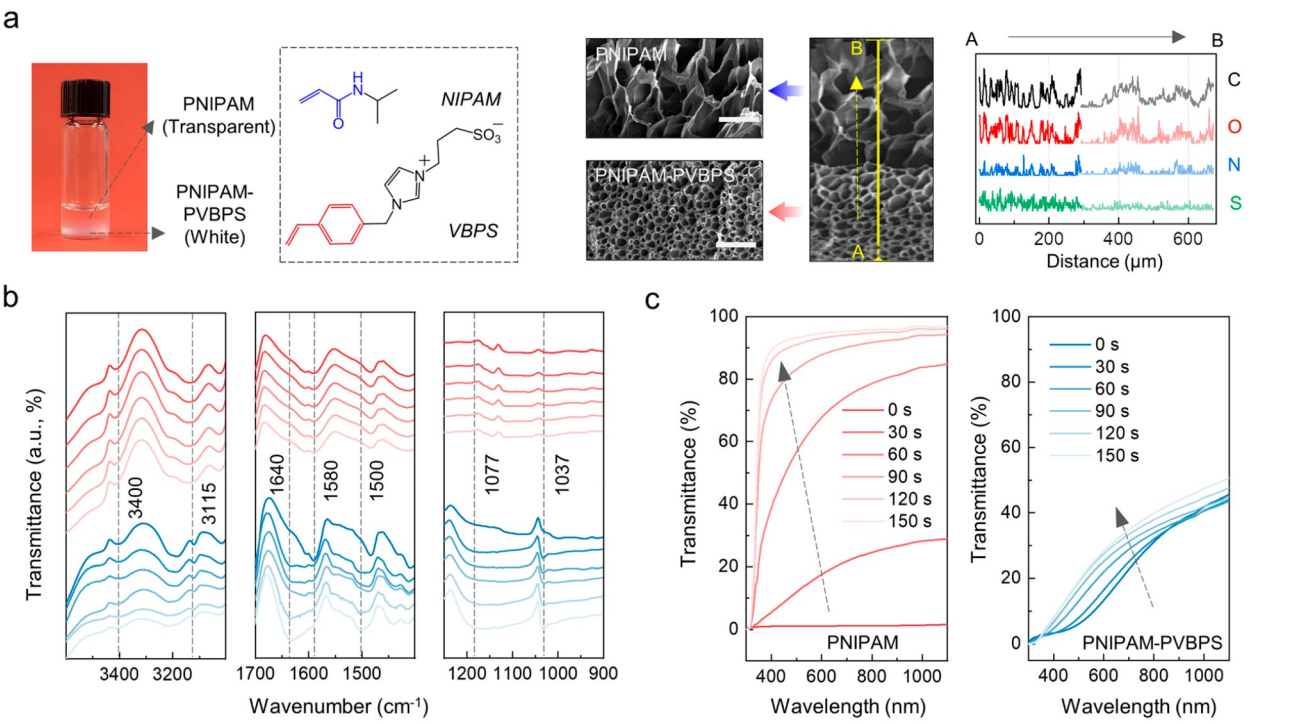

Figure 2. Structural and chemical characterizations of bilayer pNIPAM/pNIPAM-pVBPS hydrogels. (a) (left panel) Chemical structures of vinyl monomer (NIPAM) and styryl monomer (VBPS). (right panel) Interfacial characterization of bilayer pNIPAM/pNIPAM-pVBPS hydrogels by SEM images and SEM-EDS analysis of the elemental (i.e., C, N, O, S) scanning at the cross-sectional positions of A−B. Scale bar: 100 μm. (b) In situ FTIR-ATR spectra of lyophilized pNIPAM layer (red) and pNIPAM-pVBPS layer (blue) at 3600−3000, 1700−1400, and 1250−900 cm^{-1} regions to illustrate the difference of functional groups in two layers. Six different randomly selected positions for each layer were recorded for eliminating deviation. (c) Thermal-responsive transmittance variation of each layer in pNIPAM/pNIPAM-pVBPS hydrogels by UV−vis spectra in response to temperature change between 25 and 60 °C. Transmittance measurements were performed every 30 s on as-prepared hydrogels (thickness: 1 mm) sealed in a cuvette with hot water (60 °C) and until the solution temperature reached room temperature.

Both vinyl and styryl monomers possess good water solubility of >0.15 g/mL[14,15] for aqueous polymerization. Polymerized vinyl (e.g., pNIPAM) segments possessed typical thermoresponsiveness with a phase transition from hydrophilicity below LCST to hydrophobicity above LCST, while polymerized styryl network (pVBPS) containing both nitrogenous quaternary ammonium group and sulfonate group exhibits the ionic strength dependent property. The resultant pNIPAM-pVBPS bilayer hydrogels consist of a LCST layer and a polyzwitterionic layer, with the seamless interface between both layers and programmable layer thicknesses at multilength scales by controlling spontaneous macrophase separation. The macrophase separation strategy, for the first time, demonstrates a new design principle for fabricating bilayer structured materials with controllable topological networks, multiscale hierarchical structures, and stimuli-responsive functions, which provides a versatile and programmable platform for soft-smart materials and their applications.

Figure 1a shows the one-pot, macrophase separation strategy for preparing pNIPAM-pVBPS bilayer hydrogels. Specifically, all reactants consisting of 0.25 g/mL vinyl monomer (e.g., NIPAM), 0−0.1 g/mL styryl monomer (e.g., VBPS, Figure S1−3), 1.0 mg/mL cross-linker (MBAA), 3 mg/L thermal-initiator (APS), 5 mg/L photoinitiator (I-2959) were mixed and magnetically stirred in a one-pot aqueous solution at 4 °C, followed by the addition of 0.8 mg/mL accelerator (TEMED) and immediate injection of the entire precursor solution into a glass mold for further polymerization. The precursors in glass molds underwent a first thermal polymerization at 4 °C for 2−8 h, followed by sequential photopolymerization under 365 nm UV light for 2−4 h at room temperature. During the first thermal polymerization, thermal-responsive NIPAM monomers were preferentially attacked by primary radicals generated by the dianion dissociation of APS ($[O_3SO{-}OSO_3]^{2-} \rightleftharpoons 2[SO_4]^{\bullet -}$), resulting in the rapid chain growth and formation of a pNIPAM-enriched network. Meanwhile, both NIPAM and VBPS monomers will be further consumed by two representative homopolymerizations (~V$^{\bullet}$-V, ~St$^{\bullet}$-St) for homopolymer chain growth and two copolymerizations (~V$^{\bullet}$-St, ~St$^{\bullet}$-V) for random copolymeric chain growth until termination reaction occurred (Figure 1b). Since vinyl-terminated radicals usually have the lower radical reactivity than styryl-terminated radicals, V$^{\bullet}$-V and ~St$^{\bullet}$-V radical reactions rapidly formed and grew pNIPAM-enriched chains at the expense of vinyl monomers, as compared to the slow ~St$^{\bullet}$-St and ~V$^{\bullet}$-St reactions for the formation of pVBPS-enriched chains. Such a difference in radical reactions allowed both pNIPAM and pVBPS chains, which have substantial differences in molecular weight and hydrophobicity, to be separated into two layers in equilibrium with each other. Finally, pNIPAM-pVBPS bilayer hydrogels consisted of the two distinct layers of a thermal-responsive pNIPAM layer and a zwitterionic pVBPS layer, with a clear interface between them.

Since two parameters of the VBPS:NIPAM mass ratio and thermal polymerization time govern the macrophase separation behavior of bilayer hydrogels, we prepared a series of pNIPAM-pVBPS bilayer hydrogels ($V_{0-40}N_{100}$) by varying

https://doi.org/10.1021/acsmacrolett.3c00149
ACS Macro Lett. 2023, 12, 598−604

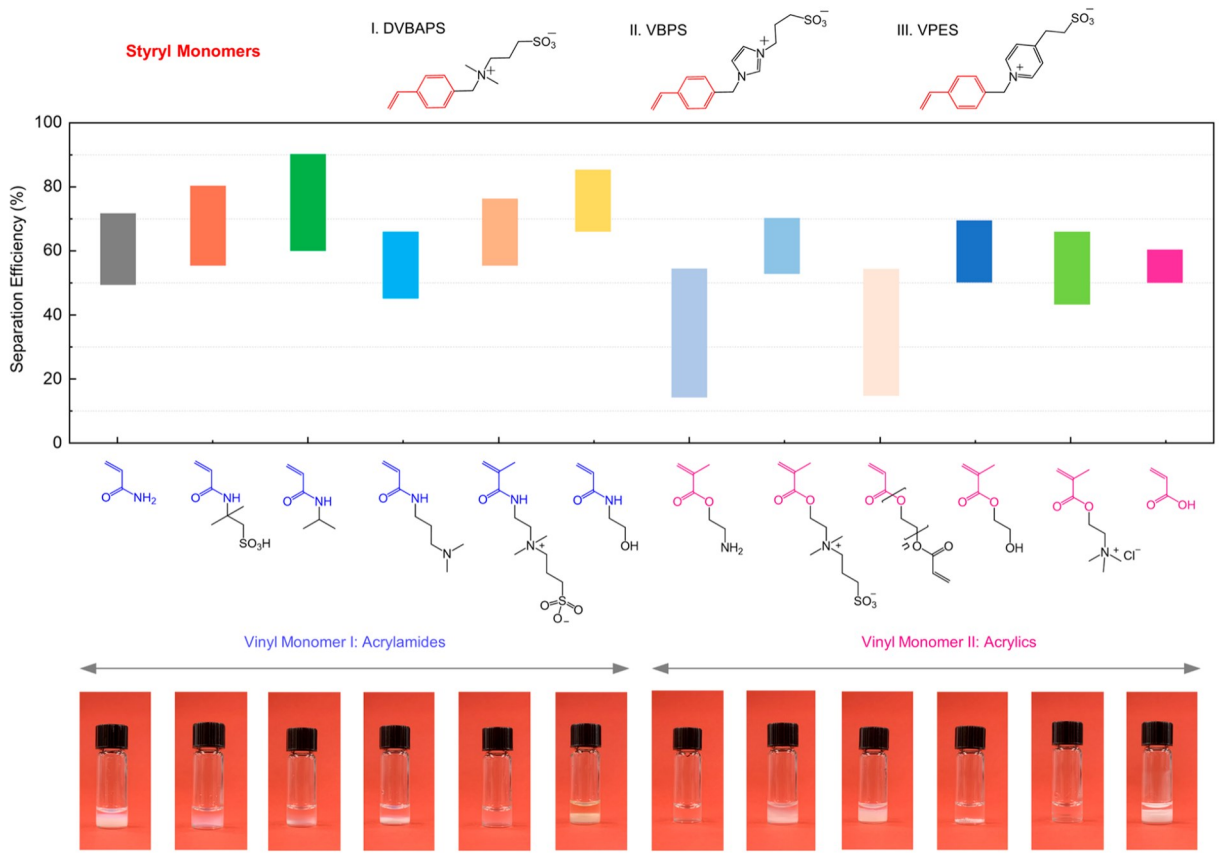

Figure 3. Macrophase-separation strategy applicable to other binary vinyl/styryl systems for the preparation of bilayer hydrogels. Comparative interlayer separation eficiencies of bilayer hydrogels made of polymeric pairs between acrylamides (AAm, AMPS, NIPAM, NDPAM, SBAA, and HEAA), acrylates (AMAH, SBMA, PEGDA, HEMA, METAC, and AAc), and styryls (DVBAPS, VBPS, and VPES). Photographs showing a series of bilayer hydrogels formed by above-mentioned vinyl monomer and VBPS pairs.

the mass ratio of VBPS:NIPAM (0:100, 10:100, 20:100, 30:100, and 40:100) and the thermal polymerization time (2.5, 3.5, 4.5, and 5.5 h). We first examined the effect of the VBPS:NIPAM ratio on the macrophase separation-induced gelation of bilayer hydrogels. It can be seen in Figure 1c that as the VBPS:NIPAM ratio increased from 0:100 to 40:100 (i.e., from 0 to 40 wt %), the resulting hydrogels showed progressively enhanced phase separation with a more pronounced bilayer structure. Visually, as compared to pure PNIPAM gels without any phase separation, the hydrogels prepared with 30−40 wt % of VBPS underwent observable phase separation from transparent to whitening over time from 2.5 to 5.5 h. So, it appears that the higher concentration of styryl monomers makes the macrophase separation much slower, as evidenced by the increased time required for the formation of a white layer from ∼1.5 h for $V_{10}N_{100}$, ∼2.5 h for $V_{20}N_{100}$, ∼3.5 h for $V_{30}N_{100}$, to ∼4.5 h for $V_{40}N_{100}$ (Figure 1d).

To understand the reactive-induced macrophase separation mechanism that governs the network disintegration during the gelation, in situ SEM-EDS was employed to characterize the interfacial and cross-sectional properties of lyophilized pNIPAM/pNIPAM-pVBPS hydrogels at nanoscale resolution. As shown in Figure 2a, the upper pNIPAM layer presented lamellar pores with relatively large pore size of 60−120 μm, while the bottom pNIPAM-pVBPS layer exhibited a denser structure, as evidenced by flat, uniform circular channels with diameters ranging from 8 to 35 μm. Such large circular channels in the bottom layer also reflect the stretching of the networks induced by macrophase separation. Further, linear elemental scanning of C, O, N, and S acquired over a cross-sectional region from A to B (0−700 μm) showed that the bottom pNIPAM-pVBPS layer covering 0−300 μm possessed the richer network abundance, as compared to the loose signal distributions in the top pNIPAM layer of 300−700 μm. Particularly, the N and S signals for amine/imidazole and sulfonate groups were mainly located in the range of 0−300 μm, but almost no S signals was detected at 300−700 μm, indicating the enrichment of pVBPS chains in the pNIPAM-pVBPS layer. Next, we applied FTIR-ATR spectra to study the network distribution of each layer in pNIPAM/pNIPAM-pVBPS hydrogels by randomly selecting six different positions (Figure S4). The bottom pNIPAM-pVBPS layer exhibited strong adsorption peaks at ∼1640, ∼1580, ∼1500, ∼1077, and ∼1037 cm^{-1}, corresponding to abundant C∼N (imidazole), aromatic rings, and sulfonate groups in the pVBPS chains. The stronger adsorption bands at 3100−3400 cm^{-1}, assigning to the higher density of hydrogen bonds, indicate the higher contents of amine groups in the upper pNIPAM layer (Figure 2b and Table S1). These results suggest that high density difference in both vinyl- and styryl-polymerized layers as made by different radical reactivities drive both networks to migrate away from the interfacial region and finally achieve spatial network separation.

We further studied the dynamic optical properties (transmittance) of two layers at different testing temperatures from 60 to 25 °C (Figure 2c). Given the thermal sensitivity of the

https://doi.org/10.1021/acsmacrolett.3c00149
ACS Macro Lett. 2023, 12, 598−604

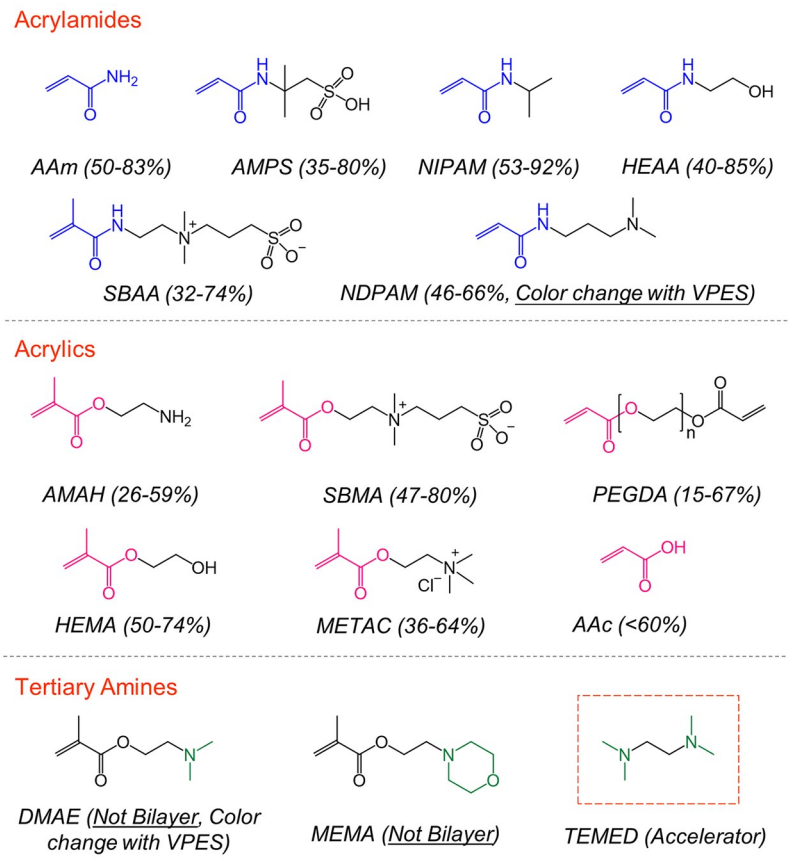

Figure 4. Comparison of the layer-separation eficiency of different vinyl monomers (6 acrylamides, 6 acrylics, and 2 tertiary amine derivatives) in the synthesis of bilayer hydrogels via reactive-induced macrophase separation.

transparent pNIPAM layer, after immersing the detached upper (pNIPAM) hydrogel layers into hot water, it immediately changed its color from transparent to opaque (i.e., ⍰0% of light transmittance) at 0 s, and its transmittance then gradually increased to ⍰20% at 30 s, ⍰70% at 60 s, ⍰85% at 90 s, ⍰92% at 120 s and thereafter. Since the pNIPAM-pVBPS layer also contained pNIPAM chains, it experienced a slight transmittance change from ⍰27% to ⍰33% under the same testing conditions. Since the swelling property is critical for stimulus-induced actuation of bilayer hydrogels, we also systematically tested and analyzed the anisotropic swelling behavior of pNIPAM layer and pNIPAM-pVBPS layer in different solutions. As shown in Figure S5, single-layer pNIPAM-pVBPS hydrogels (⍰154 wt %) exhibited a relatively higher swelling rate than single-layer pNIPAM hydrogels (⍰115 wt %) in water. Such a higher swelling rate of pNIPAM-pVBPS hydrogels is probably stemmed from the higher density of porous channels in styryl-enriched network, consistent with morphologically porous structures in SEM images. Differently, both layers containing pVBPS chains swelled less in water than in 0.1 M NaCl solution, because zwitterionic pVBPS chains possessed antipolyelectrolyte effect, in which zwitterionic polymers tended to adopt stretched conformations in salt solution due to ionic solvation, resulting in 1.5-fold increase in the swelling ratio (up to ⍰250 wt %) as compared to the pNIPAM layer (⍰169 wt %). Taken together, a substantial difference in swelling, transmittance, and morphology in both layers again confirms the reactive-induced macrophase separation of pNIPAM-pVBPS hydrogels into the two distinct microdomain structures in equilibrium with each other.

To further verify whether our reactive-induced macrophase separation strategy is applicable to other polymeric systems, we designed and synthesized a family of bilayer hydrogels, mainly covering different combinations of polymerized styryl-based monomers (VBPS, DVBAPS, and VPES) and vinyl-based monomers (acrylamides of AAm, AMPS, NIPAM, NDPAM, SBAA, and HEAA and acrylates of AMAH, SBMA, PEGDA, HEMA, METAC, and AAc) (Table S2 and Figure 3). Specifically, due to the presence of vinyl groups with low steric hindrance in acrylamide-based monomers (AAm, AMPS, NIPAM, NDPAM, SBAA, and HEAA), acrylamide-based monomers generally have higher free radical reactivity than styryl-based monomers to facilitate chain growth, which subsequently enhances the macrophase separation of the two polymerized networks. Quantitatively, we define separation eficiency by measuring the visible thickness and comparing functional group distributions with FTIR-ATR spectra. For all tested acrylamides-styryl-based binary systems, regardless of side chain characteristics (monomeric polarity, hydrogen bonding acceptor/donor sites, and chain flexibility), they can be sequentially polymerized and separated into bilayer structures with well-defined delamination interface and high interlayer separation eficiency of 48−90%. Unlike acrylamides, during the one-pot polymerization of acrylates and styryl monomers, not all of acrylate-styryl-based binary systems can be gelled to form bilayer hydrogels. Evidently, some acrylate monomers of SBMA, HEMA, METAC, and AAc contain a very high intrinsic reactivity assigned importance to strong electron-donating and hydrogen-bonding groups (e.g., quaternary ammonium, hydroxyl),[16] so they exhibited the faster

https://doi.org/10.1021/acsmacrolett.3c00149
ACS Macro Lett. 2023, 12, 598−604

polymerization rate than styryl monomers, and the greater polymerization rates also led to the early reduction in termination of acrylate monomers due to polar effects. Afterward, the initial and growth reactions of styryl monomers were allowed to proceed, followed by the macrophase separation to form bilayer structures with comparable separation eficiency of 45−70%.[17−19] However, for AMAH and PEGDA monomers have more active terminate groups (e.g., primary amine group and dual vinyl group), whose radical structures were stabilized by intramolecular hydrogen bonds between amine group and ester group. Highly reactivity in AMAH and PEGDA enabled rapid gelation, which restricts the diffusion/sedimentation channels of styryl monomers, eventually resulting in low separation eficiency of 20−35%. A solution to this highly cross-linked issue was to reduce the monomer concentration of AMAH and PEGDA below 0.15 g/mL. In this way, the resultant pAMAH-pVBPS and PEGDA-pVBPS hydrogels largely improved their separation eficiencies from <30% to 52% and from ⍰20% to 40%, respectively (Figure 4). Overall, compared with acrylamide-styryl-based bilayer hydrogels, acrylate-styryl-based hydrogels exhibit a strong structure-dependent bilayer structure formation and interlay separation eficiency, presumably because the presence of ester bonds attached to α-hydroxymethyl instead of methyl sterically hinder the free radical propagation, thereby affecting their initial gelation and subsequent macrophase separation.

It is also interested to observe that some acrylamides or acrylates (e.g., DMAE, MEMA) containing tertiary amide groups, which have a similar backbone structure to a gelling accelerator (TEMED), are likely to cause reaction implosion and instantaneous gelation, thereby resulting in the formation of uniform bulk hydrogels with extremely low separation eficiencies of <10% (yellow-green color, Table S2). Given that the structural diversity of different vinyl monomers and styryl monomers, our findings provide important structural insights into how subtle structural changes of pendent groups (amide, ester, ethylene glycol groups) in vinyl and styryl monomeric pairs control radical reactions and gelation processes for preparing a variety of bilayer hydrogels via spontaneous macrophase separation. This study identified a family of vinyl- and styryl-based monomer pairs that are reactively compatible to enable one-pot gelation, while still retaining suficient physicochemical difference for allow macrophase (spatial network) separation, which have not been achieved before.

Developing new fabrication strategies and identifying suitable radical polymers to realize bilayer hydrogels is an exciting fundamental challenge from the viewpoint of material design to delivery. Here, we report a general macrophase separation strategy and a pool of vinyl and styryl monomers for the fabrication of a new family of bilayer hydrogels. Through careful screening and control the rate of free radical polymerization between hydrophilic vinyl and styryl monomers, a series of monomeric acrylamides-styryl (AAm/VBPS, AMPS/VBPS, NIPAM/VBPS, NDPAM/VBPS, SBAA/VBPS, and HEAA/VBPS) and acrylates-styryl (AMAH/VBPS, SBMA/VBPS, PEGDA/VBPS, HEMA/VBPS, METAC/VBPS, and AAc/VBPS) pairs were identified to achieve bilayer hydrogels with seamless interfaces by one-pot, radical reaction-induced macrophase separation. There are two key points in the working principle of the macroscopic phase separation strategy, the first is to make the two monomer pairs suficiently compatible for sequential but independent free-radical polymerizations in a one-pot solution, while the second key point is that during the gelation process, the two formed networks should be significant differences in physicochemical property, thereby achieving delamination. Thanks to the structural diversity of available vinyl and styryl monomers with different radical reactivity, the macrophase separation strategy allows to construct a pool of bilayer hydrogels with tunable interlayer separation eficiency of 20−90%. Our macrophase separation strategy produces a seamless interface between the two layers. This structural integrity allows for superior spatiotemporal actuations in response to external stimuli, such as shape transformation, movements, bending, and twisting. HEAA/VBPS, PEGDA/VBPS, NIPAM/VBPS, and AAc/VBPS even exhibited antifreezing property at −20 °C. Additionally, this approach enables the creation of programmable bilayer hydrogels for specific applications. For example, (i) bilayer hydrogels can be used to deliver drugs to specific sites in the body, where the top layer can be designed to release the drug, while the bottom layer is used to control the rate of diffusion into the surrounding tissue; (ii) bilayer hydrogels can be used to engineer tissues by mimicking the structure and function of tissues, where the top layer mimics the epidermis, while the bottom layer mimics the dermis; (iii) bilayer hydrogels can be used to promote wound healing by providing a scaffold for tissue regeneration, in which the top layer is designed to absorb exudate, while the bottom layer is used to support tissue growth under a moist environment for healing; (iv) bilayer hydrogels can be used as biosensors by incorporating enzymes/antibodies in the top layer as probes, while the bottom layer serves as an adhesion layer to attach to any sensor substrate. Overall, the seamless interface of our bilayer hydrogels offers structural and functional advantages that can lead to improved performance in various fields, while the one-pot, macrophase separation strategy demonstrates a new design principle and a pool of radical monomers for fabricating bilayer hydrogels with controllable topological networks beyond few available today.

ASSOCIATED CONTENT

* Supporting Information

The Supporting Information is available free of charge at https://pubs.acs.org/doi/10.1021/acsmacrolett.3c00149.

Methods (materials and characterizations), ^{1}H NMR spectra of styryl monomers, FTIR spectra, mass swelling ratio curves for pNIPAM layer and pNIPAM-pVBPS layer, assignment of bands in curve resolved FTIR spectra of studied PNIPAM/PNIPAM-PVBPS bilayer hydrogels, and photos of reactive-induced bilayer hydrogels prepared in this work (PDF)

AUTHOR INFORMATION

Corresponding Author

Jie Zheng − *Department of Chemical, Biomolecular, and Corrosion Engineering, The University of Akron, Akron, Ohio 44325, United States;* orcid.org/0000-0003-1547-3612; Email: zhengj@uakron.edu

Authors

Dong Zhang − *Department of Chemical, Biomolecular, and Corrosion Engineering, The University of Akron, Akron, Ohio 44325, United States;* orcid.org/0000-0001-7002-7661

https://doi.org/10.1021/acsmacrolett.3c00149
ACS Macro Lett. 2023, 12, 598−604

Yijing Tang − *Department of Chemical, Biomolecular, and Corrosion Engineering, The University of Akron, Akron, Ohio 44325, United States*
Xiaomin He − *Hangzhou Singclean Medical Products Co., Ltd., Hangzhou 310018, China*
William Gross − *Department of Chemical, Biomolecular, and Corrosion Engineering, The University of Akron, Akron, Ohio 44325, United States*
Jintao Yang − *College of Materials Science and Engineering, Zhejiang University of Technology, Hangzhou 310014, China;* orcid.org/0000-0002-3133-1246
Complete contact information is available at: https://pubs.acs.org/10.1021/acsmacrolett.3c00149

Author Contributions

J.Z. supervised this project. D.Z. and J.Z. conceived the concepts. D.Z. and Y.T. designed the research, synthesized all bilayer hydrogels, and conducted characterizations. D.Z., X.H., J.Y., and J.Z. discussed the reactive-induced macrophase separation in binary monomer system for bilayer hydrogels. D.Z. and J.Z. wrote the paper. All authors discussed the results and commented on the manuscript. CRediT: Xiaomin He formal analysis (equal), methodology (equal), validation (equal); William Gross data curation (equal), formal analysis (equal), validation (equal); Jie Zheng conceptualization (lead), funding acquisition (lead), project administration (lead), supervision (lead), writing-original draft (lead), writing-review & editing (lead).

Funding

This work was supported by NSF (2311985) and ACS-PRF-65277.

Notes

The authors declare no competing financial interest.

REFERENCES

(1) Yue, Y. F.; Kurokawa, T.; Haque, M. A.; Nakajima, T.; Nonoyama, T.; Li, X. F.; Kajiwara, I.; Gong, J. P. Mechano-actuated ultrafast full-colour switching in layered photonic hydrogels. *Nat. Commun.* 2014, *5* (1), 1−8.
(2) Li, M. T.; Wang, X.; Dong, B.; Sitti, M. In-air fast response and high speed jumping and rolling of a light-driven hydrogel actuator. *Nat. Commun.* 2020, *11* (1), 1−10.
(3) Zhang, K.; Oldenhof, S.; Wang, Y.; Esch, J. H.; Mendes, E. Spatial Manipulation and Integration of Supramolecular Filaments on Hydrogel Substrates towards Advanced Soft Devices. *Angew. Chem., Int. Ed.* 2020, *59* (22), 8601−8607.
(4) Yang, J. J.; Zhang, X. F.; Zhang, X.; Wang, L.; Feng, W.; Li, Q. Beyond the Visible: Bioinspired Infrared Adaptive Materials. *Adv. Mater.* 2021, *33* (14), 2004754.
(5) Li, C.; Xue, Y. G.; Han, M. D.; Palmer, L. C.; Rogers, J. A.; Huang, Y. G.; Stupp, S. I. Synergistic photoactuation of bilayered spiropyran hydrogels for predictable origami-like shape change. *Matter* 2021, *4* (4), 1377−1390.
(6) Mredha, M. T. I.; Jeon, I. Biomimetic anisotropic hydrogels: Advanced fabrication strategies, extraordinary functionalities, and broad applications. *Prog. Mater. Sci.* 2022, *124*, 100870.
(7) Zhang, F.; Lian, M.; Alhadhrami, A.; Huang, M.; Li, B.; Mersal, G. A.; Ibrahim, M. M.; Xu, M. Laccase immobilized on functionalized cellulose nanofiber/alginate composite hydrogel for efficient bisphenol A degradation from polluted water. *Advanced Composites and Hybrid Materials* 2022, *5*, 1852−1864.
(8) Kong, D.; El-Bahy, Z. M.; Algadi, H.; Li, T.; El-Bahy, S. M.; Nassan, M. A.; Li, J.; Faheim, A. A.; Li, A.; Xu, C.; Huang, M.; et al. Highly sensitive strain sensors with wide operation range from strong MXene-composited polyvinyl alcohol/sodium carboxymethylcellulose double network hydrogel. *Advanced Composites and Hybrid Materials* 2022, *5*, 1976−1987.
(9) Hua, J.; Bjorling, M.; Larsson, R.; Shi, Y. Friction Control of Chitosan-Ag Hydrogel by Silver Ion. *ES Materials & Manufacturing* 2021, *16*, 30−36.
(10) Jian, Y.; Wu, B.; Yang, X.; Peng, Y.; Zhang, D.; Yang, Y.; Qiu, H.; Lu, H.; Zhang, J.; Chen, T. Stimuli-responsive hydrogel sponge for ultrafast responsive actuator. *Supramolecular Materials* 2022, *1*, 100002.
(11) Shim, T. S.; Kim, S. H.; Heo, C. J.; Jeon, H. C.; Yang, S. M. Controlled Origami Folding of Hydrogel Bilayers with Sustained Reversibility for Robust Microcarriers. *Angew. Chem. Int. Edit* 2012, *51* (6), 1420−1423.
(12) Yao, C.; Liu, Z.; Yang, C.; Wang, W.; Ju, X. J.; Xie, R.; Chu, L. Y. Smart Hydrogels with Inhomogeneous Structures Assembled Using Nanoclay-Cross-Linked Hydrogel Subunits as Building Blocks. *Acs Appl. Mater. Inter* 2016, *8* (33), 21721−21730.
(13) Rong, M.; Ma, S.; Lin, P.; Cai, M.; Zheng, Z.; Zhou, F. Polymerization induced phase separation as a generalized methodology for multi-layered hydrogel tubes. *J. Mater. Chem. B* 2019, *7* (22), 3505−3511.
(14) Zhang, D.; Tang, Y.; Zhang, C.; Huhe, F.; Wu, B.; Gong, X.; Chuang, S. S. C.; Zheng, J. Formulating Zwitterionic, Responsive Polymers for Designing Smart Soils. *Small* 2022, *18* (38), 2203899.
(15) Zhang, D.; Tang, Y.; Yang, J.; Gao, Y.; Ma, C.; Che, L. B.; Wang, J.; Wu, J.; Zheng, J. De novo design of allochroic zwitterions. *Mater. Today* 2022, *60*, 17−30.
(16) Degirmenci, I.; Avcı, D.; Aviyente, V.; Van Cauter, K.; Van Speybroeck, V.; Waroquier, M. Density Functional Theory Study of Free-Radical Polymerization of Acrylates and Methacrylates: Structure−Reactivity Relationship. *Macromolecules* 2007, *40* (26), 9590−9602.
(17) Carter, S.; Hunt, B.; Rimmer, S. Highly branched poly(N-isopropylacrylamide)s with imidazole end groups prepared by radical polymerization in the presence of a styryl monomer containing a dithioester group. *Macromolecules* 2005, *38* (11), 4595−4603.
(18) Zhang, D.; Tang, Y. J.; Zhang, Y. X.; Yang, F. Y.; Liu, Y. L.; Wang, X. Y.; Yang, J. T.; Gong, X.; Zheng, J. Highly stretchable, self-adhesive, biocompatible, conductive hydrogels as fully polymeric strain sensors. *Journal of Materials Chemistry A* 2020, *8* (39), 20474−20485.
(19) Zhang, D.; Liu, Y. L.; Liu, Y. H.; Peng, Y. P.; Tang, Y. J.; Xiong, L. M.; Gong, X.; Zheng, J. A General Crosslinker Strategy to Realize Intrinsic Frozen Resistance of Hydrogels. *Adv. Mater.* 2021, *33* (42), 2104006.